https://doi.org/10.31436/iiumej.v27i3.4276

Digital Twin Framework for Integrated Sequential Laser Beam Micromachining (LBMM) and Micro-EDM

Wan Ahmad Bin Wan Azhar[1], Tanveer Saleh[1*], Khairul Affendy Bin Md Nor[2], Muhammad Mukhtar Bin Noor Awalludin[3], Abd Halim Bin Embong[1], Ali Sophian[1], Mohd Asyraf Bin Mohd Razib[1], Azhar Bin Mohd Ibrahim[2]

[1]Autonomous Systems and Robotics Research Unit, Department of Mechatronics Engineering, International Islamic University Malaysia, 53100, Jalan Gombak, Kuala Lumpur, Malaysia
[2]Department of Mechatronics Engineering, International Islamic University Malaysia, 53100, Jalan Gombak, Kuala Lumpur, Malaysia
[3]Department of Manufacturing and Materials Engineering, International Islamic University Malaysia, 53100, Jalan Gombak, Kuala Lumpur, Malaysia

**Corresponding author: tanveers@iium.edu.my*

(Received: 17 March 2026; Accepted: 30 July 2026; Published online: 11 September 2026)

ABSTRACT: Micro-hole arrays are widely used in aerospace, biomedical devices, and filtration applications. While many methods exist for producing these arrays, achieving high precision, efficiency, and low cost in a single process remains challenging. An integrated sequential method combining Laser Beam Micromachining (LBMM) for fast material removal and micro Electrical Discharge Machining (μEDM) for precise finishing offers a promising solution. However, the sequential operation of these two processes presents challenges such as collision risk, coordination difficulties, and monitoring limitations. To address these issues, this paper proposes a Digital Twin (DT) framework integrated with the Internet of Things (IoT) for real-time analysis and decision-making, which improves process coordination, collision-aware operation, and virtual validation of sequential LBMM–μEDM machining. The DT enables real-time monitoring by leveraging accurate 3D geometries of machine components to enhance the realism and precision of collision detection. The virtual 3D representation was developed using Unity3D software, while IoT connectivity for real-time data exchange was established through Firebase, resulting in an average transmission latency of 16 ms. The DT eliminates the need for live camera feeds by enabling flexible, low-bandwidth, multi-angle visualization without extra hardware, while also supporting offline virtual simulations for motion coordination, realistic cutting effects, and machining time estimation with a 79.8% prediction accuracy.

ABSTRAK: Susunan lubang mikro digunakan secara meluas dalam pelbagai aplikasi seperti aeroangkasa, peranti bioperubatan dan sistem penapisan. Walaupun pelbagai kaedah pemesinan telah dibangunkan untuk menghasilkan susunan lubang ini, pencapaian ketepatan tinggi, kecekapan proses serta kos pengeluaran yang rendah secara serentak masih menjadi satu cabaran. Kaedah pemesinan berjujukan yang menggabungkan pemesinan mikro pancaran laser bagi menyingkirkan bahan secara pantas dan pemesinan nyahcas elektrik mikro bagi membuat kemasan berketepatan tinggi, berpotensi menjadi satu penyelesaian berkesan. Namun, pelaksanaan kedua-dua proses secara berjujukan menimbulkan beberapa cabaran seperti risiko perlanggaran antara komponen mesin, kesukaran dalam penyelarasan proses serta keterbatasan pemantauan operasi. Sehubungan itu, kajian ini mencadangkan satu rangka kerja kembar digital yang diintegrasi bersama teknologi Internet Kebendaan bagi menyokong analisis masa nyata dan pembuatan keputusan, membolehkan penyelarasan proses dengan lebih baik, operasi berasaskan pengesanan perlanggaran, serta pengesahan maya bagi pemesinan berjujukan LBMM–µEDM. Rangka kerja kembar digital yang dicadangkan membolehkan pemantauan masa nyata melalui penggunaan model geometri tiga dimensi komponen mesin yang tepat, sekaligus meningkatkan tahap realisme dan ketepatan dalam pengesanan perlanggaran. Persekitaran maya tiga dimensi dibangun menggunakan perisian pembangunan grafik tiga dimensi, manakala sambungan Internet Kebendaan bagi pertukaran data masa nyata dilaksanakan melalui pangkalan data awan, dengan purata kelewatan penghantaran data direkodkan sebanyak 16 milisaat. Selain itu, sistem kembar digital yang dibangunkan dapat menggantikan keperluan penggunaan kamera langsung dengan menyediakan visualisasi berbilang sudut yang fleksibel serta penggunaan jalur lebar yang rendah tanpa memerlukan perkakasan tambahan. Sistem ini juga menyokong simulasi maya secara luar talian bagi tujuan penyelarasan pergerakan mesin, visualisasi kesan pemotongan yang realistik serta penganggaran masa pemesinan dengan ketepatan ramalan sebanyak 79.8%.

KEYWORDS: *Digital Twin; Sequential Hybrid Machining, Laser Beam Micromachining (LBMM); Micro Electrical Discharge Machining (µEDM); Real-time Monitoring; Collision Detection.*

1. INTRODUCTION

In advanced engineering applications, a micro hole array is a patterned grid or arrangement of repetitive micro-scale holes created on a material surface to serve structural, fluidic, optical, or functional purposes. They play a vital role in numerous industries because of their versatile functional advantages. In the aerospace sector, they are used to cool turbine blades under high temperatures [1]. In water filtration systems, these arrays improve the detection of trace heavy metals [2]. In the field of microfluidics, ceramic-based arrays facilitate accurate fluid control [3].

Despite their importance, producing high-precision, repeatable micro-hole arrays remains a manufacturing challenge. Various fabrication methods are used to create these structures, including electrochemical machining (ECM), micro-EDM, laser drilling, and mechanical punching. ECM provides high surface quality without tool wear but requires precise parameter control [4]. Micro-EDM (µEDM) is suitable for hard, conductive materials and achieves excellent accuracy, though it is slow and limited in material types [5]. Laser drilling offers fast, contactless processing but can cause thermal damage [6]. Mechanical punching is productive but struggles with miniaturization and alignment [7]. The choice of method depends on the material, feature size, and intended application.

Researchers have investigated various approaches to enhance micromachining efficiency by integrating different machining techniques. The core concept of hybrid machining involves combining two or more machining methods or principles to overcome the limitations of standalone processes and achieve superior component quality and performance. For instance, in laser-assisted micro-milling, laser preheating softens the workpiece, thereby improving material removal rates up to six times and extending tool lifespan [8]. One of the most promising hybrid approaches combines laser beam micromachining (LBMM) with micro-EDM (µEDM) in sequence. In this method, LBMM is used for rapid roughing to reduce material volume, minimize thermal damage, and limit recast-layer formation, followed by µEDM for fine surface quality and precise dimensions. Studies have shown that this combined method reduces processing time for fuel injector nozzles by up to 70% while maintaining high hole quality at diameters below 145 µm [9]. In some cases, hole drilling times dropped by 90% for 125–130 µm diameter holes compared to conventional µEDM alone [10].

Despite the advantages of hybrid or sequential machining processes, several challenges remain, with collision risk during setup and operation being a major concern. Hybrid setups often involve multiple machining heads, increasing the potential for collisions. This risk is especially significant in computer-aided manufacturing (CAM), where simulations may not account for all physical components such as clamps or vices [11]. Some CAM software simulates only toolpaths or material removal, ignoring fixture geometry, which can result in undetected collisions during actual machining. Chen et al. (2017) also noted that in hybrid additive–subtractive processes, improperly planned material heights can prevent cutting tools from reaching certain areas, causing collisions [12]. This issue is particularly critical in sequential LBMM–μEDM systems, where multiple heads operate in a confined space alongside components such as the workpiece holder and dielectric tank.

Another critical challenge in hybrid machining is coordinating and sequencing different machining stages. Basinger et al. (2019) highlighted this issue in their development of the Feature-based Advanced Hybrid Process Planning System (FAH-PS), which automates process planning using feature-specific geometric and material data [13]. Their study showed that manual process planning often takes weeks because of these coordination complexities, whereas the FAH-PS achieved a 35% reduction in machining time in a patient-specific bone plate case study. Furthermore, the complexity of coordination and sequencing in hybrid machining also affects operator training. Operators need to understand both additive and subtractive processes, which makes the learning process longer and more difficult [14]. In the sequential LBMM–μEDM system, operators must be well trained in both processes, as any mistake in sequencing, tool alignment, or parameter setup can affect machining accuracy and overall process efficiency.

Monitoring machining processes using live camera feeds presents several limitations. Although they provide real-time visuals, cameras are restricted to fixed viewpoints. They are often obstructed by cutting fluids or debris, making it challenging to inspect hidden or critical areas during operation [15]. Expanding camera coverage requires additional hardware, increasing both system complexity and cost. Furthermore, live video streaming demands high bandwidth and may experience latency or degraded quality, especially under high-resolution or remote monitoring conditions [16]. These challenges highlight the need for advanced solutions such as Digital Twin (DT) technology to enhance monitoring, coordination, sequencing, and collision detection in sequential LBMM–μEDM processes.

A Digital Twin (DT) is a virtual representation of a physical system that continuously mirrors its real-time behavior using 3D models, positional data, sensor information, and control parameters. Unlike a digital model, which is static and requires manual updates, or a digital shadow, which supports only one-way data flow from the physical to the virtual system, a DT enables bi-directional communication, allowing both physical and virtual entities to exchange information in real time for predictive analysis, optimization, and autonomous decision-making [17]–[19]. In manufacturing, DT provides a comprehensive 3D visualization of the machining environment, including machine components, tool heads, workpieces, and fixtures, enabling process planning, collision detection, operation sequencing, and performance optimization. When integrated with the Internet of Things (IoT), DT also supports remote monitoring and virtual operator training without requiring access to the physical machine. DT platforms are commonly developed using tools such as Siemens TIA Portal, Unity, Game4Automation, MATLAB/Simulink, and ANSYS Twin Builder for real-time visualization, control integration, and physics-based simulation.

A recent DT application in machining is the prediction and compensation of thermal-induced time-varying errors in CNC machine tool axes, where a time-varying error model based on heat transfer theory and a visual model was used [20]. This approach effectively predicted and compensated for errors, reducing hole-pitch fluctuation by 69.19%, demonstrating the potential of DT in enhancing machining accuracy and performance. In contrast, a novel DT framework was developed to support offline robotic EDM cutting-path programming by simulating tool kinematics and addressing complex issues such as collisions and singularities. This approach enhances the integration of industrial robots with EDM for the precise machining of hard-to-cut materials [21].

This paper proposes a Digital Twin (DT) framework integrated with the Internet of Things (IoT) for real-time analysis and decision-making. This study aims to develop a DT framework integrated with IoT technology to support sequential machining processes, improving process coordination, collision-aware operation, and virtual validation of sequential LBMM–µEDM machining. The framework addresses critical challenges in hybrid and sequential machining, particularly collision risk, process coordination, and real-time monitoring. By leveraging 3D geometric models of the LBMM head, µEDM head, and surrounding fixtures, the DT enables real-time monitoring and enhances collision detection throughout the machining operations, without relying on live camera systems. In addition, the framework simulates coordination and sequencing between different machining stages, enabling users to plan and monitor operations more efficiently. This work also contributes to operator training by offering a virtual platform for observing and understanding process flows and interactions, eliminating the need for physical machines or on-site presence.

2. DIGITAL TWIN SYSTEM ARCHITECTURE

This section details the system architecture and framework of the digital twin for the sequential LBMM-µEDM process, including the physical machine, related software, IoT implementation, DT virtual representation, and the Unity-based user interface.

2.1. Integrated LBMM-µEDM Physical Setup

The physical setup integrates LBMM and µEDM processes into a single system, as illustrated in Figure 1. In this configuration, the LBMM module is mounted horizontally offset from the µEDM unit, while the workpiece remains fixed within the µEDM workspace and is accessible to both processes. The LBMM system employs a 50W fiber laser (1060 nm wavelength, 50 µm spot size, 200 mm focal length) driven by an X/Y galvanometer scanner with a ±15° scan range and 12 µrad resolution. Laser output was calibrated using a Gentec Pronto-250 power meter, which records the average output power. Calibration was performed from 10% to 100% laser setting. Although rated at 50 W, the measured output at 100% was approximately 38.6 W, indicating a power loss of about 22.8%. This reduction is consistent with the laser supplier's specifications and is attributed to transmission losses through multiple optical components, such as collimators, beam expanders, mirrors, and the galvanometric scanner. Each optical component contributes to reflection, scattering, or absorption losses, reducing the power delivered to the workpiece surface. A calibration curve was generated to correlate the percentage setting with the actual delivered power. For this experiment, the laser was operated at 90%, corresponding to a calibrated output of 35.4 W. The laser head is height-adjustable via a rotary mechanism and traverses horizontally on a motorized linear stage, while EZCAD Lite software controls the process parameters.

The µEDM subsystem consists of a three-axis CNC machine with a repeatability of 15 µm, equipped with a µEDM spindle and a microscopic camera mounted on the Z-axis plate. Custom control software provides camera visualization, parameter configuration, G-code execution, and real-time axis monitoring. The process flow and sequence are illustrated in Figure 2. Initially, as shown in Figure 2(a), the LBMM head extends over the workpiece to perform laser machining while the μEDM head remains retracted in a safe position. Once the LBMM process is completed, the laser head retracts to allow for the subsequent μEDM operation.

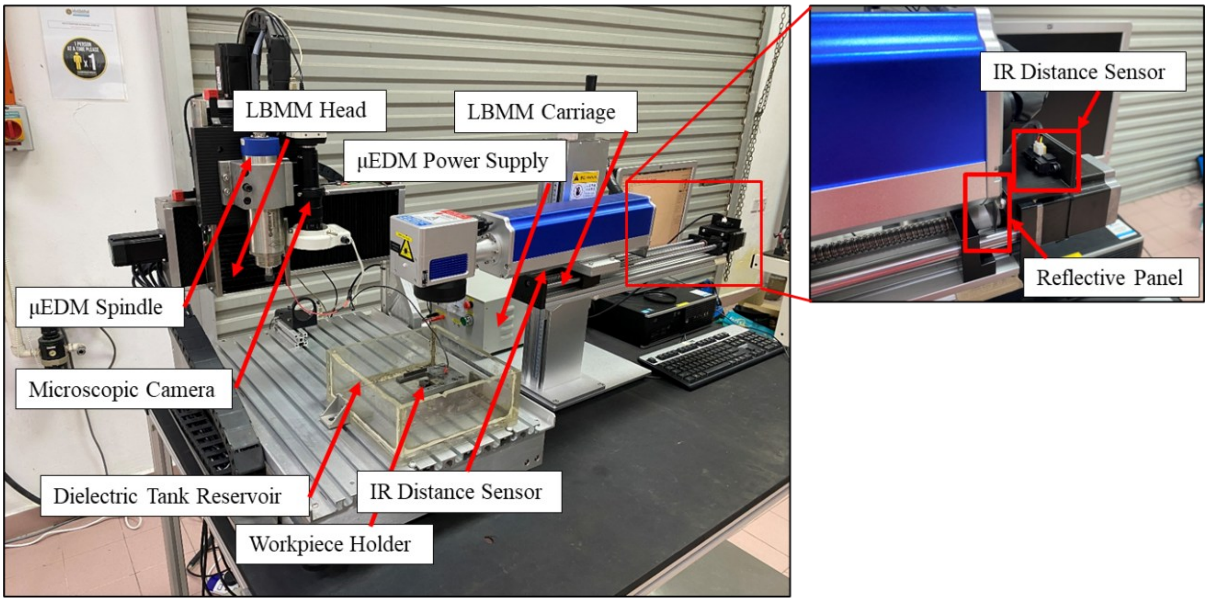

Figure 1. Physical setup of the hybrid Laser Beam Micromachining (LBMM) and micro-EDM (μEDM) system, showing the integrated configuration used for sequential machining operations on a shared workpiece.

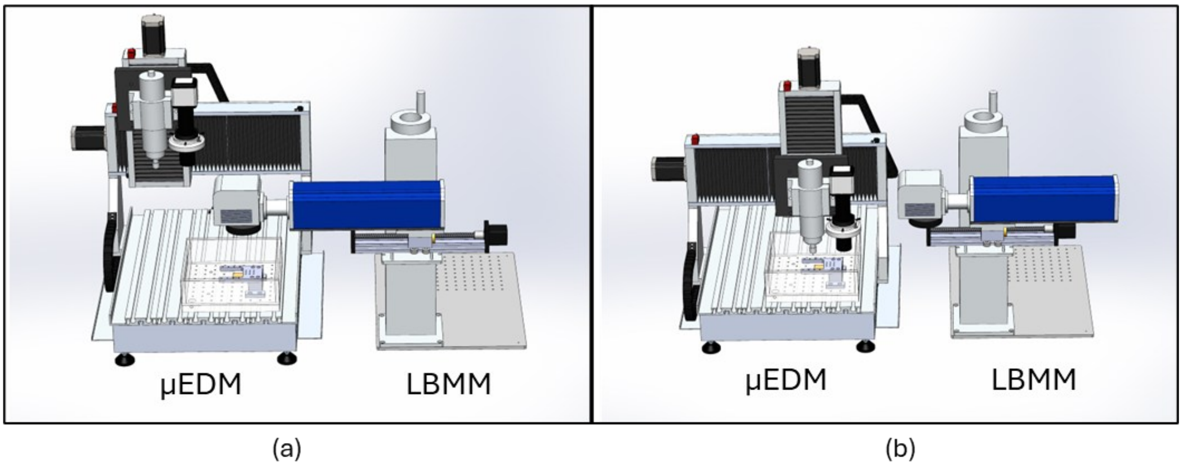

Figure 2. Machine Configuration (3D model):
(a) During the LBMM process; (b) During the μEDM process.

The position of the LBMM carriage is monitored using an infrared (IR) distance sensor (model: GP2D120XJ00F), as illustrated in Figure 1, which operates effectively within a measurement range of 0–30 cm. The sensor has a typical response time of approximately 39 ms, with output sensitivity decreasing from ~0.12 V/mm at shorter distances to ~0.025 V/mm at longer distances. Next, the μEDM head, equipped with a spindle, a microscopic camera, and a ring light, advances toward the workpiece. This operation is illustrated in Fig.2(b). The microscopic camera that is mounted on the Z-axis is used to localize the LBMM-machined holes and determine their center coordinates, as described in a previous study [22]. After

https://doi.org/10.31436/iiumej.v27i3.4276

verifying the coordinates, μEDM power supply parameters such as gap voltage, capacitance, discharge and short thresholds, and polarity are configured. Subsequently, the software automatically generates the G-code for the μEDM fine finishing process, enabling a fully coordinated and automated machining sequence. The changeover between the two processes takes approximately 36 seconds. The LBMM and μEDM Parameters, and IR sensor specifications are tabulated in Table 1.

Table 1. LBMM and μEDM Parameters, and IR Sensor specifications.

LBMM Parameters	
Loop Count	75
Programmed Diameter (μm)	180
Scanning Speed (mm/s)	10
Laser Rated Power (W)	50
Actual Measured Laser Power (W)	38.6
Applied Laser Power (W)	35.4 (or 90%)
Frequency (Khz)	50
Hatch Angle (°)	0
Line Space (mm)	0.01
Focal Spot Size (μm)	50
Hatch Type	Two-way Hatch 
μEDM Parameters	
Power Supply Type	Resistor- Capacitor (RC)
Resistance (KΩ)	1
Electrode Material	Tungsten
Electrode Diameter (μm)	300
Workpiece Material	Stainless Steel (SUS304)
• Thermal Conductivity (W/m-K)	16.2
• Melting Point (°C)	1400 - 1455
• Electrical Resistivity (μΩ·m)	0.72
Workpiece Thickness (μm)	200, 400 and 600
Gap Voltage (V)	90
Capacitance (nF)	10 (1.8 Stray Cap)
Discharge Energy (μJ)	40.5
Spindle Speed (RPM)	1200
Feedrate (μm/s)	5
Flushing Method	Atmospheric Pressure
Dielectric Fluid	Mineral-based EDM oil
Polarity	Workpiece: Positive Tool: Negative

For validation purposes, a stainless steel (SS304) plate with dimensions of 20 mm × 20 mm and thicknesses of 200 μm and 600 μm was used. A cylindrical tungsten electrode with a 300 μm diameter was chosen because of its high thermal wear resistance and low tool wear rate. The machining process involved creating an array of three LBMM pilot micro-holes in a single row, evenly spaced 1 mm apart, followed by fine finishing of the through-holes using μEDM with a 300 μm diameter tungsten electrode (as available in the lab). The LBMM pilot-hole size plays an important role in achieving efficient and high-quality machining. A hole that is too small restricts tool access during μEDM, increasing machining time, while an overly large hole increases the extent of HAZ, recast layer, and spatter, which can degrade final feature quality. To balance these factors, preliminary trials were conducted to identify an appropriate pilot-hole size that provides both effective LBMM performance and efficient µEDM finishing. The LBMM process parameters were selected based on the optimization performed in our previous study [23]. Each LBMM pilot hole had an average entry and exit diameter of approximately 200 µm and 100 µm, respectively, residual spatter of 280 µm, and a HAZ extending up to 470 µm.

2.2. Integrated LBMM-µEDM Physical Setup

Figure 3 illustrates the Digital Twin (DT) framework developed for the unified Laser Beam Micromachining (LBMM) and Micro Electrical Discharge Machining (µEDM) setup. In this integrated system, the LBMM process is managed through EZCAD software, while the µEDM process is controlled via custom-developed µEDM CNC controller software. Both systems communicate through serial interfaces, enabling coordinated operation and seamless data exchange.

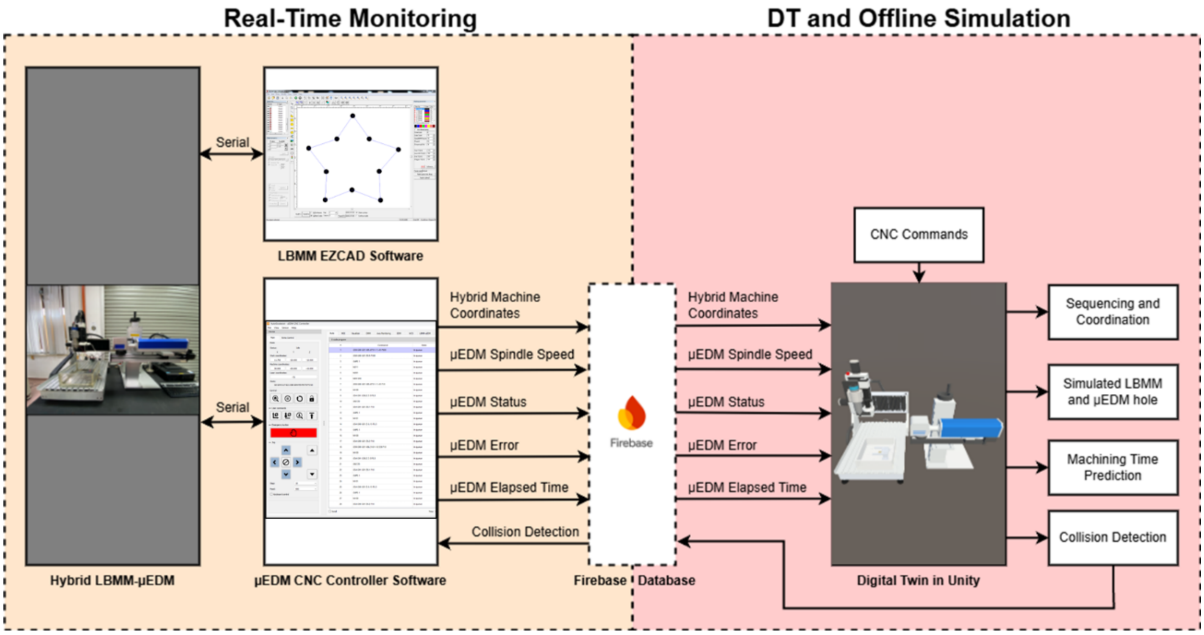

Figure 3. Digital Twin (DT) framework for the unified LBMM-µEDM setup, illustrating both real-time monitoring and offline simulation modes.

For the LBMM process, EZCAD software controls key laser parameters such as scanning speed, frequency, loop count, LBMM carriage position, and other settings crucial to achieving the desired machining accuracy. In addition, an infrared (IR) distance sensor tracks the position of the LBMM carriage. This positional data is sent to the µEDM CNC Controller, enabling synchronization between the LBMM and µEDM stages for improved coordination in the integrated setup.

For the µEDM CNC machine, a customized control software named *the µEDM CNC Controller was developed by modifying the open-source CANDLE software,* written in C++ using the Qt5 framework. This software has been extensively enhanced to manage µEDM power supply parameters, including gap voltage, RC circuit capacitance, discharge and short-circuit thresholds, and voltage polarity. In addition, it controls the CNC motion system and implements an automatic retraction mechanism that holds the position upon discharge and retracts to clear shorts when detected. The µEDM CNC controller executes G-code toolpaths and includes real-time X, Y, and Z plotting for process monitoring. Additionally, on-machine

https://doi.org/10.31436/iiumej.v27i3.4276

measurement (OMM) and automation features were integrated to streamline the transition between LBMM and µEDM processes, enabling seamless and efficient sequential operation.

Furthermore, Firebase Realtime Database integration was implemented to support bidirectional data exchange, enabling real-time remote monitoring and seamless synchronization with the digital twin environment in Unity. This data includes the machine coordinates, µEDM spindle speed, µEDM status and error messages, and µEDM elapsed time.

Unity3D, functioning as the DT platform, continuously receives and processes real-time data from the µEDM CNC system. One critical DT function is collision detection, which is available in both real-time and simulation modes. When a potential collision is detected based on position and the 3D model, the system sends a warning signal back to Firebase. The µEDM CNC controller monitors this signal and promptly halts machine motion to prevent any damage. For safety, no control commands are sent through Firebase, and only monitoring and warning functions are enabled. This ensures that the µEDM CNC controller software remains securely isolated from unauthorized or accidental external operations. A subsequent section explains the detailed logic for collision detection, collider setup, and Unity implementation.

The Digital Twin for the sequential LBMM-µEDM system operates in two modes: real-time mode for live monitoring and collision detection, and simulation mode for offline process planning and visualization. In real-time mode, Figure 4(a) depicts the Unity3D interface with a live 3D visualization of the machine. The machine's position is dynamically updated based on data received from Firebase, allowing users to accurately monitor tool and workpiece movement. A status panel shows the current process state, error messages, and elapsed machining time. A camera control panel enables users to switch between predefined views, zoom in and out, and rotate the scene to observe operations from different perspectives. This flexibility makes it useful for monitoring and offers advantages over live camera feeds, which are limited by fixed viewpoints and potential obstructions. Real-time collision warnings are indicated visually when a collision is detected.

The system also includes a simulation mode, as illustrated in Figure 4(b), for offline testing and process planning. In this mode, users can input CNC commands using a dedicated G-code panel, with options to write, load, and save code files. Once the simulation runs, the virtual machine follows the programmed toolpath, showing animated motion and hole-generation sequences for both LBMM and µEDM. The visual logic for the hole-cutting simulation is detailed in the following section. A reset button allows users to restart the simulation. The system calculates and displays estimated machining time based on feedrate and delay values defined in the G-code. However, for a more realistic estimation, the simulation incorporates actual µEDM Z-displacement data to account for the additional µEDM processing time.

The DT is entirely software-based and requires no additional hardware. All machines have existing 3D models that can be directly imported into Unity3D for simulation and visualization. Unity3D is the environment used to develop the digital twin (DT). While the Personal plan is free for individual use, the Pro plan is available at USD 200 per month per seat for professional development. The system also requires an internet connection and uses Firebase for data storage and communication. Firebase pricing depends on the selected plan and usage level. Under typical operating conditions, expenses are minimal, as the free Spark plan supports moderate data storage and real-time updates, while the Blaze plan offers a pay-as-you-go option for higher usage. Overall, this approach is highly cost-effective compared to hardware-based solutions.

https://doi.org/10.31436/iiumej.v27i3.4276

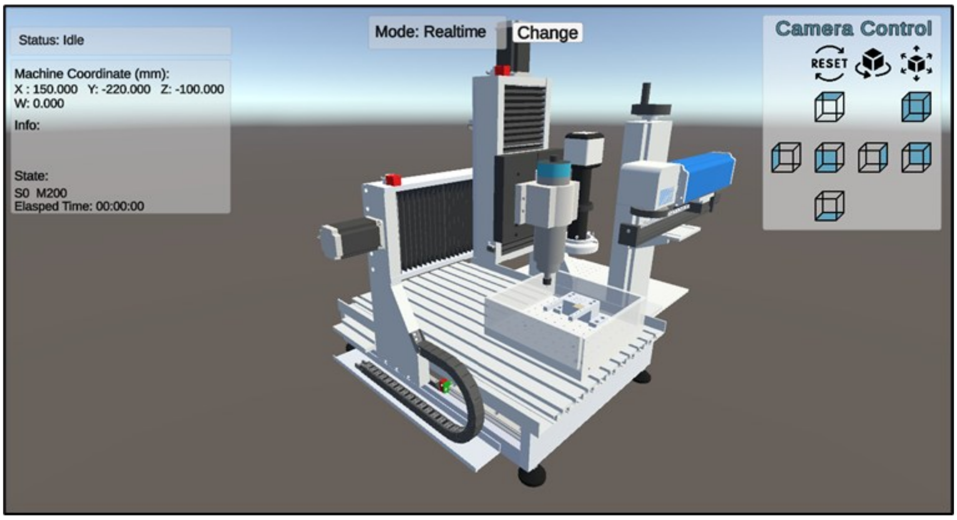

(a)

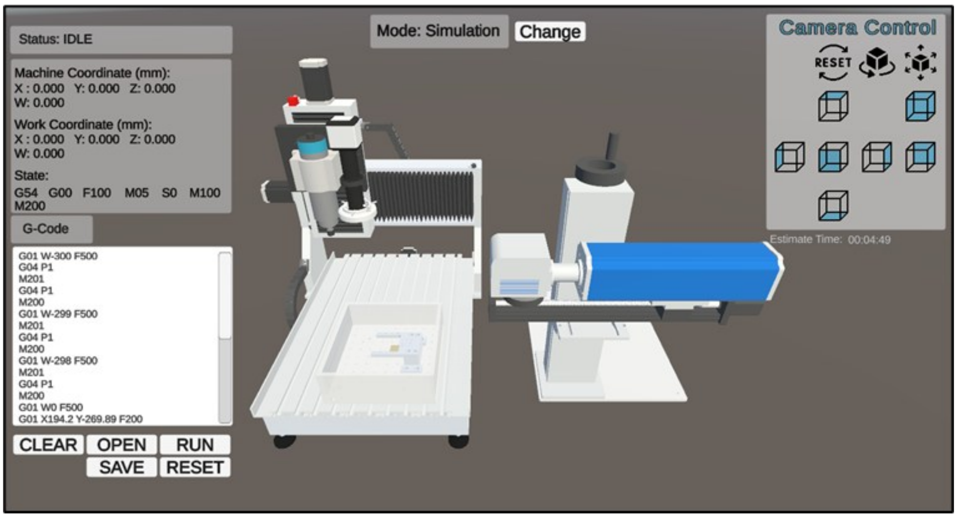

(b)

Figure 4. GUI Interfaces of the Digital Twin System. (a) Real-time mode GUI displaying live machine position updates from Firebase, µEDM process status, error alerts, elapsed time, and camera control panel for view navigation. (b) Simulation mode GUI featuring G-code editor, run/reset controls, estimated machining time display, and animated toolpath with hole cutting simulation for both LBMM and µEDM processes.

3. DIGITAL TWIN FOR REAL-TIME MONITORING WITH COLLISION DETECTION

This section presents the implementation of a Digital Twin for real-time monitoring, including online simulation and integrated collision detection. It is divided into three parts: Section 3.1 describes real-time monitoring, Section 3.2 describes the setup and components of the collision detection system, and Section 3.3 discusses latency results and system response, evaluating the effectiveness and responsiveness of the safety mechanism during operation.

3.1. Real-time Monitoring

To demonstrate the effectiveness of the DT during actual LBMM–µEDM operation, a machining experiment was performed. In this test, the LBMM created 200 µm pilot holes in a 200 µm-thick stainless steel (SS304) workpiece, which were subsequently enlarged and finefinished to 300 μm using the μEDM process. A total of three holes were machined. The complete sequence of the physical machine workflow and its corresponding DT operations is illustrated in Figure 5.

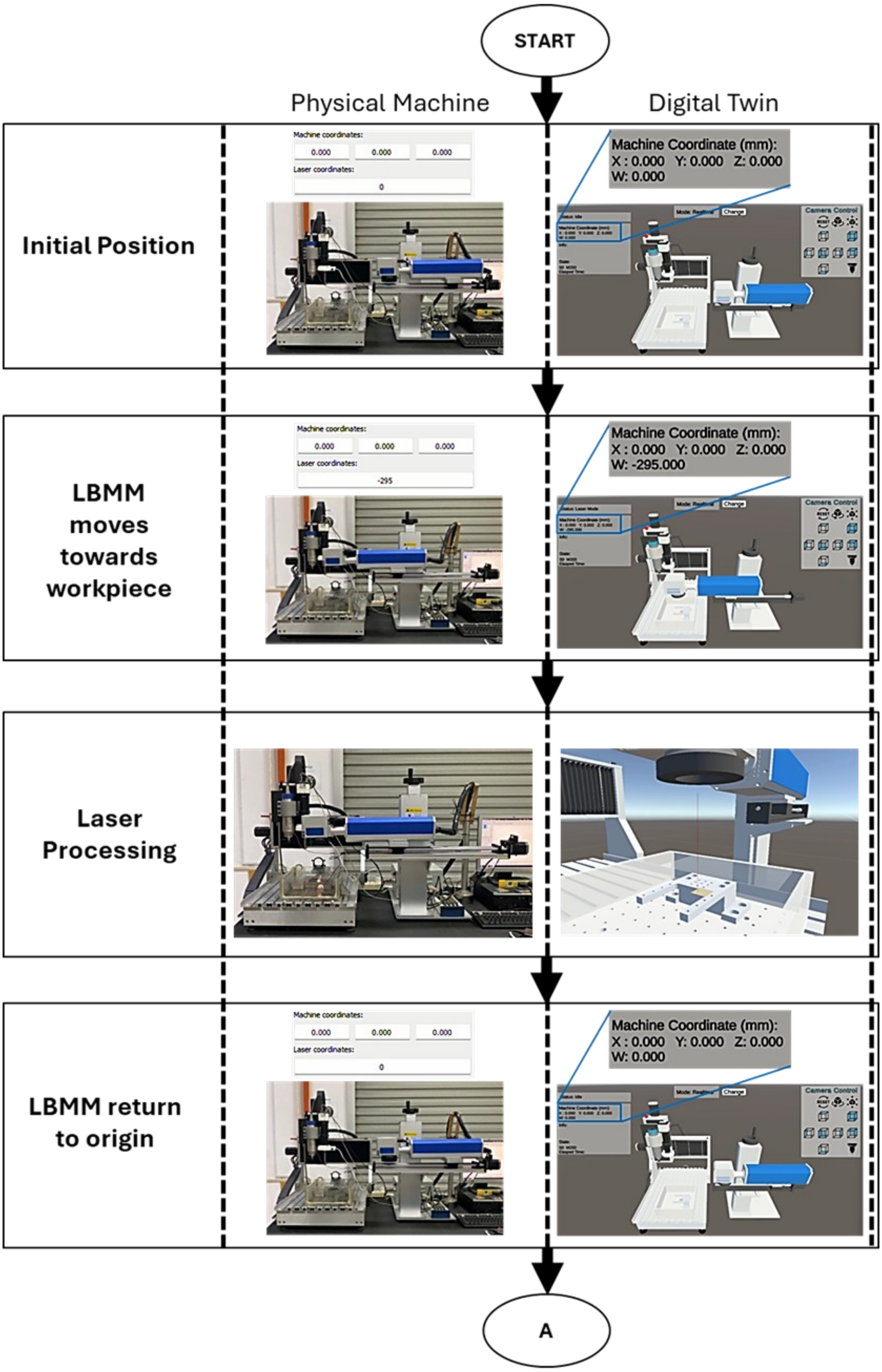

(a)

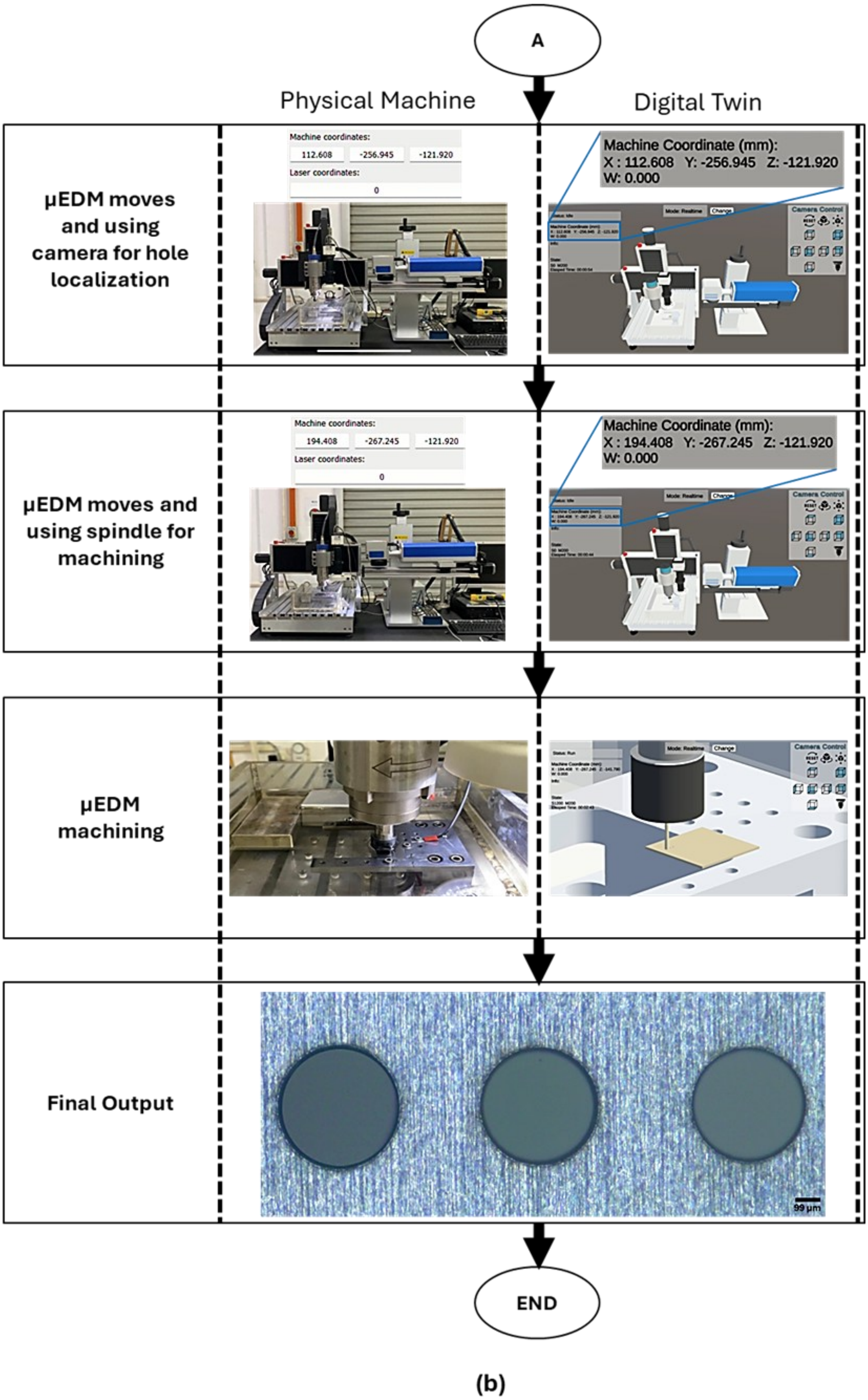

Figure 5. Flowchart of the integrated sequential LBMM–µEDM machining process, showing both the physical machine operations and the corresponding Digital Twin (DT) updates: (a) Initial position and LBMM operations, (b) µEDM operations, including hole localization, spindle positioning, and final output.

The process begins with both modules at their initial positions, as illustrated in Figure 5(a). The LBMM head then moves toward the workpiece and performs the laser machining operation. After completing laser processing, the LBMM returns to its origin to allow the µEDM head to proceed. The µEDM head unit subsequently moves forward, where the camera system is utilized to localize the LBMM-drilled pilot hole and determine its precise coordinates for the fine-finishing stage. The µEDM Z-axis is equipped with both a camera for LBMM hole localization and a spindle for the actual µEDM machining, each serving a distinct function. Once localization is completed, the µEDM head moves to the identified position, and the µEDM process is carried out, as shown in Figure 5(b). The DT continuously tracks machine motions and matches the coordinate values between the µEDM CNC controller software (physical system) and the DT throughout the sequence.

3.2. Collision Detection System Setup

This section outlines the setup and components of the collision detection system. The primary components being monitored are the µEDM head (comprising the spindle, microscopic camera, and ring light), the LBMM head, the dielectric tank reservoir, and the workpiece holder. The collision detection mechanism relies on continuous monitoring of the 3D geometries and distances between these components within a virtual environment. To achieve accurate real-time collision detection, the system employs Unity3D's Box Collider components, which are assigned to the respective monitoring elements. In Unity3D, colliders detect physical interactions, with common types including box, cylinder, sphere, and capsule colliders. The Box Collider was selected because its simple geometric structure reduces computational load and enables faster, more efficient collision detection in real-time simulations. Each Box Collider defines the geometric boundary of its corresponding physical component. In addition, a dynamic safety offset, ranging from 5 mm to 10 mm depending on the feed rate or motion speed, is applied to facilitate early collision detection before physical contact occurs. As shown in Figure 6 (a) and (b), green box colliders represent the µEDM head, and blue represents the other monitoring components. Unlike conventional point-based or bounding-box proximity checks, this method uses well-positioned 3D box colliders that reflect the actual tool and machine geometry, enhancing the realism and accuracy of collision detection. When the tool's collider intersects with another component's collider, the DT sends a signal to the µEDM CNC controller through Firebase, prompting an immediate halt in machine movement, effectively preventing mechanical damage.

This shape-based awareness is particularly useful in complex regions of the machine, such as the dielectric tank reservoir, where confined space and irregular geometry present higher risks. For instance, when the µEDM tool approaches from outside the dielectric tank reservoir, the collision detection system triggers as the tool's box collider intersects with the tank's box collider, as shown in Figure 7 (a) and (b). Additionally, within the confined space of the tank, the system effectively detects potential collisions between the tool and the workpiece holder, as illustrated in Figure 8 (a) and (b), showcasing the system's ability to ensure safe operations in both open and confined environments.

Proper machine architecture and motion planning should minimize collision risk without heavy reliance on real-time detection. The proposed Digital Twin-based collision detection provides additional safety during manual jogging and setup, which is especially beneficial during alignment operations where tool movements are unpredictable and require live feedback. The same monitoring system also runs during automated G-code machining, providing continuous protection throughout the full operation.

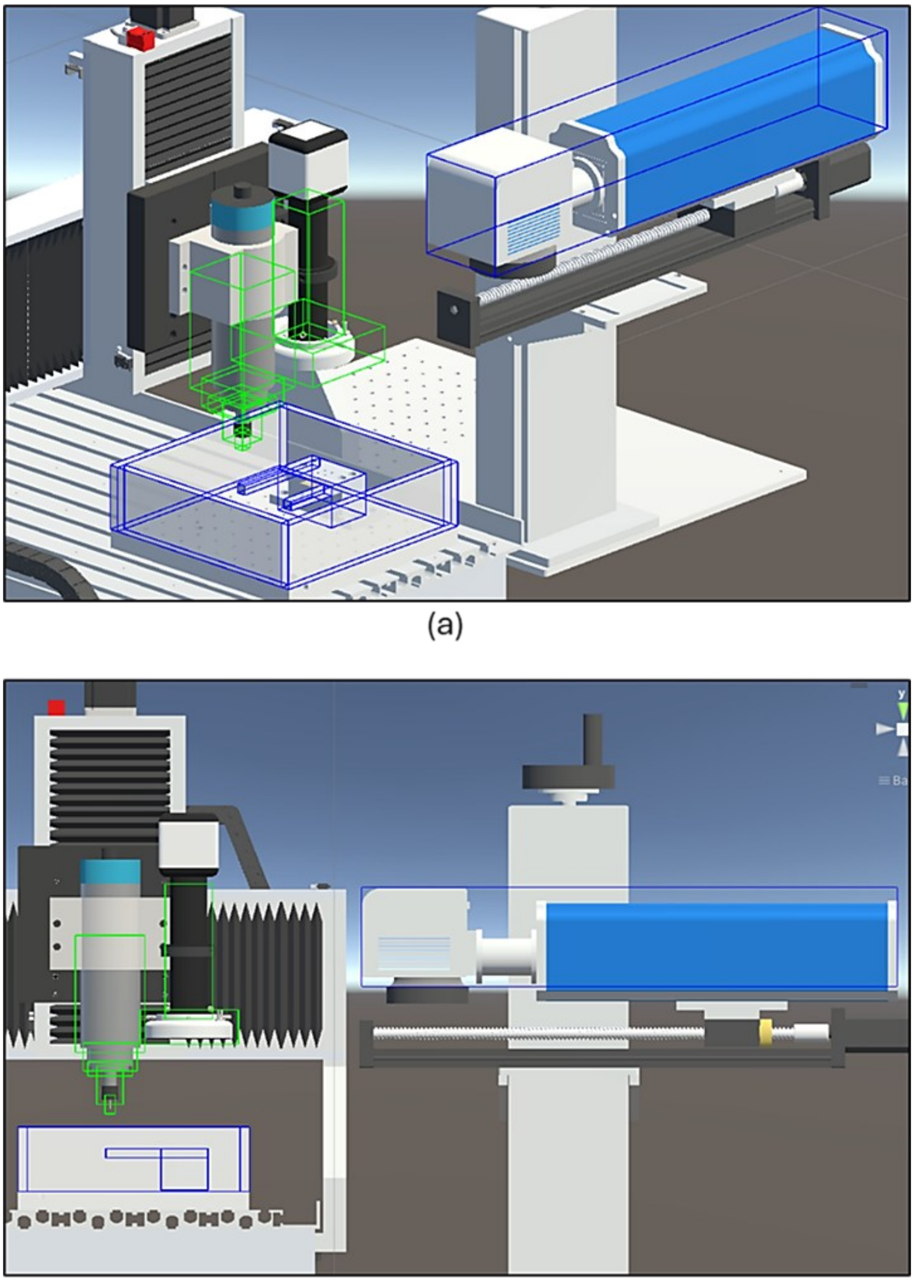

(a)

(b)

Figure 6. Box colliders with safety offset used for collision detection. Green box colliders represent the µEDM head, while blue box colliders represent other monitoring components. (a) Isometric view, (b) Side view.

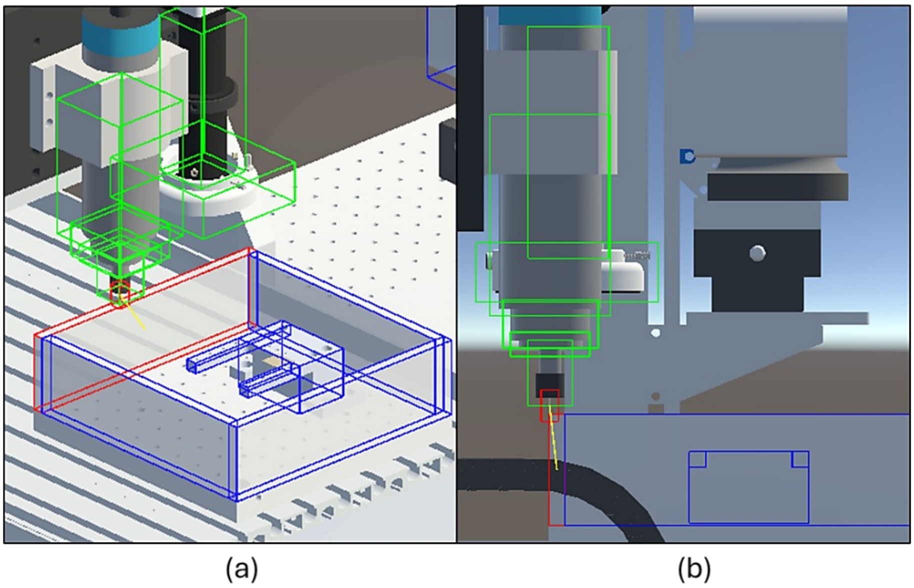

Figure 7. Collision detection (with safety offset) between the tool and the dielectric tank reservoir. (a) Isometric view, (b) Side view. Green box colliders represent the tool, blue box colliders represent the dielectric tank and workpiece holder, and red areas indicate detected collisions.

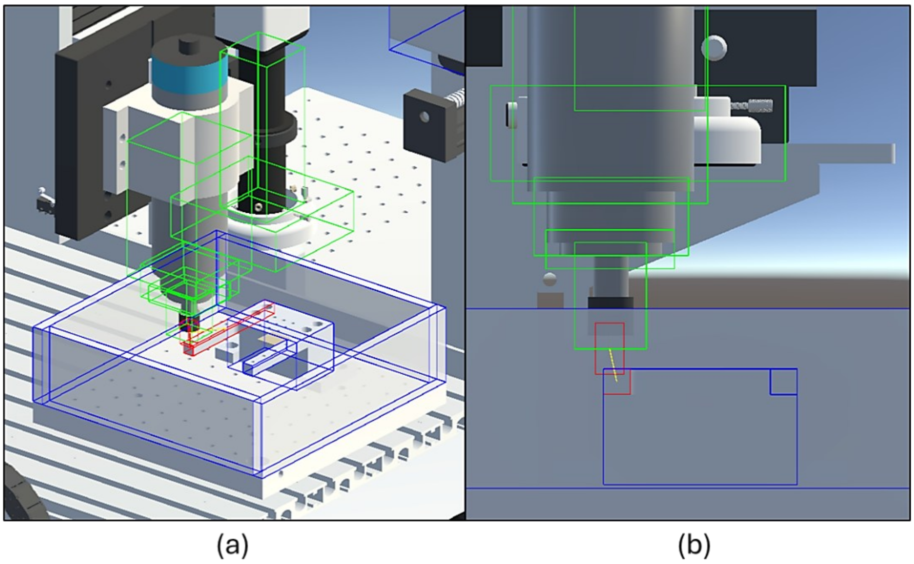

Figure 8. Collision detection (with safety offset) between the tool and the workpiece holder. (a) Isometric view, (b) Side view. Green box colliders represent the tool, blue box colliders represent the workpiece holder and dielectric tank, and red areas indicate detected collisions.

3.3. Latency and System Response

To evaluate the real-time responsiveness of the Digital Twin system, a latency test measured the time delay between issuing a movement command from the µEDM CNC control software and the corresponding position update in the Unity-based visualization interface. Two critical timestamps were recorded: (1) when the command was sent from the control software, and (2) when the updated tool position was visually reflected in Unity. The test was repeated ten times to ensure consistency and reliability. The results, illustrated in Figure 9, showed an average latency of approximately 16 milliseconds, with the maximum recorded latency being 19 milliseconds. This low delay confirms the system's capability to provide near-instantaneous feedback, which is essential for effective real-time monitoring and collision detection.

Compared to other Digital Twin (DT)-based monitoring systems that achieve synchronization rates of around one second [37], the proposed system demonstrates a significantly faster response time, making it better suited to time-sensitive industrial applications. Latency remained stable across all test iterations, indicating the robustness of the communication pipeline. The DT eliminates the need for live camera feeds by enabling flexible, low-bandwidth, multi-angle visualization without added hardware costs.

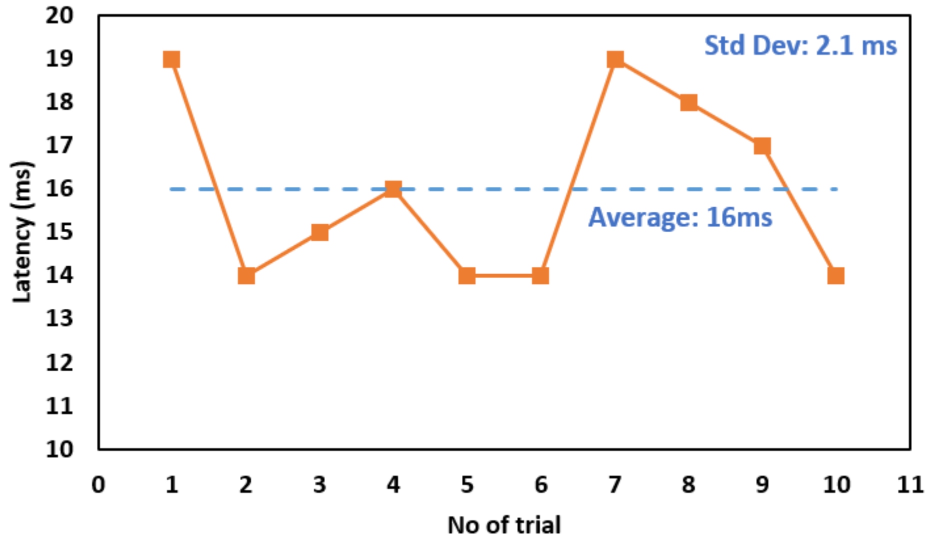

Figure 9. Latency Measurement for Real-Time Digital Twin System

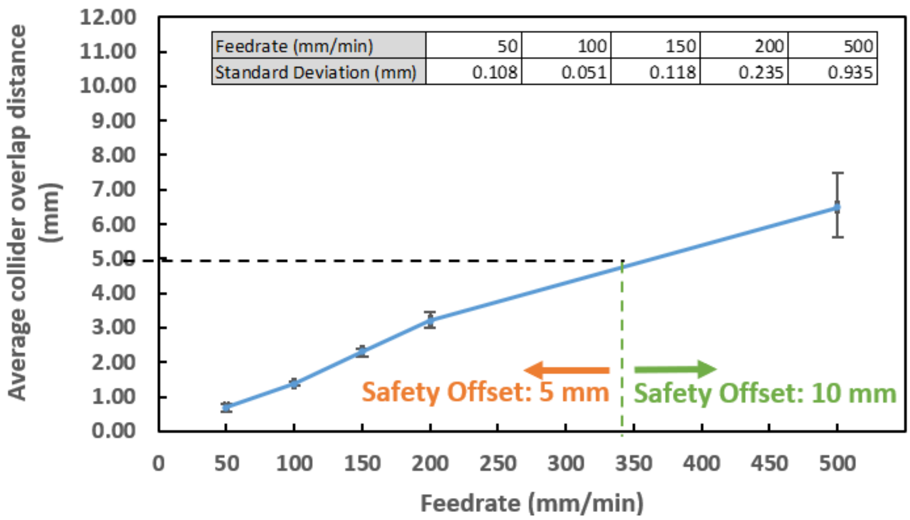

Figure 10. Average collider overlap distance at different feed rates (n = 3) with error bars representing the minimum and maximum values observed for each feed rate.

In the context of machine, workpiece, and tool motion, latency refers to the time delay between issuing a command and the system's corresponding physical response. This delay must be accounted for in the control strategy so that, when a halt signal is issued, the tool decelerates appropriately and does not overshoot or collide with the workpiece. In this work, a dynamic safety offset, ranging from 5 mm to 10 mm depending on the feed rate or motion speed, is applied to facilitate early collision detection before physical contact occurs. To further validate this approach, experiments were conducted at different feed rates, with a 5 mm safety offset. The experiment involves moving the µEDM tool toward the dielectric tank along the Y-axis (as in Figure 10) at feed rates of 50, 100, 150, 200, and 500 mm/min. The resulting collider overlap distances were recorded three times for each feed rate and are presented in Figure 10. The collider overlap distance increases with feed rate, as higher feed rates result in greater momentum, requiring a longer distance for the tool to decelerate safely. At a feed rate of 500 mm/min, the measured overlap of 6.5 mm exceeds the default safety offset of 5 mm. Based on linear interpolation, feed rates of 350 mm/min and above also surpass the 5 mm safety offset. Therefore, for feed rates above 350 mm/min, the DT system will automatically adjust the safety offset to 10 mm to ensure the tool stops in time and avoids contact with the dielectric tank.

4. DIGITAL TWIN FOR OFFLINE PROCESS COORDINATION

This section discusses the use of the Digital Twin system for offline simulation and planning of the sequential LBMM–µEDM machining process. It highlights the system's ability to interpret G-code and M-code commands and simulate tool movements and process coordination. Section 4.1 demonstrates how tool and workpiece interactions, such as hole formation during LBMM or µEDM, are visually represented in the Unity environment. Meanwhile, Section 4.2 focuses on the system’s ability to estimate machining time based on G-code feed rates and interpolated real µEDM process data, providing predictive insights to support process planning.

4.1. CNC Command Simulation with Visualized Cutting Effects

In simulation mode, the Digital Twin was tested for its ability to accurately interpret and execute a variety of standard CNC commands commonly used in CNC machining operations. It utilizes the same set of commands as the actual µEDM CNC controller, ensuring consistency between the virtual simulation and real-world execution. The supported commands are tabulated in Table 2. These M-codes are not standard ISO or FANUC codes and apply only to this system, where they are custom-defined and may vary between manufacturers.

Table 2. List of supported CNC Commands on the DT for offline simulation

CNC Command	Description
G0, G01	Rapid and linear interpolation movement (X,Y,Z,W)
G90, G91	Absolute and incremental positioning
G38.2	Probing command for surface detection
G04	Dwell command for pause simulation
G10 L20	Work offsets G54 to G59
M03, M04, M05	Spindle control (clockwise, counterclockwise, stop)
M200, M201	Laser ON/OFF commands
M101, M100	µEDM simulation ON/OFF commands

In addition, in the Digital Twin environment, the interaction between the machining tools and the workpiece is simulated using visual cues that mimic material removal. When the LBMM laser beam or the µEDM electrode engages with the workpiece, the system creates see-through or hollow areas on the simulated workpiece mesh to illustrate the cutting or drilling effect. For instance, when the LBMM beam interacts with the surface, a 300 µm diameter hole is visualized, while µEDM operations produce a 500 µm diameter hole, reflecting the size of the tungsten electrode used. Figure 11(a) shows an example where a 300 µm LBMM hole is first created, followed by larger 500 µm µEDM holes at the same position, as shown in Figure 11(b), illustrating the sequential machining process. These visualized effects allow users to intuitively verify the cutting sequence and assess potential errors or collisions in an offline environment. The workpiece is modeled using a ProBuilder mesh in Unity, and hole generation is implemented through mesh subtraction library [38]. In this process, the volume of the

LBMM beam or the μEDM tool is subtracted from the workpiece mesh, effectively simulating material removal. This approach creates realistic visual effects, with holes appearing at the exact locations where the tool interacts with the workpiece.

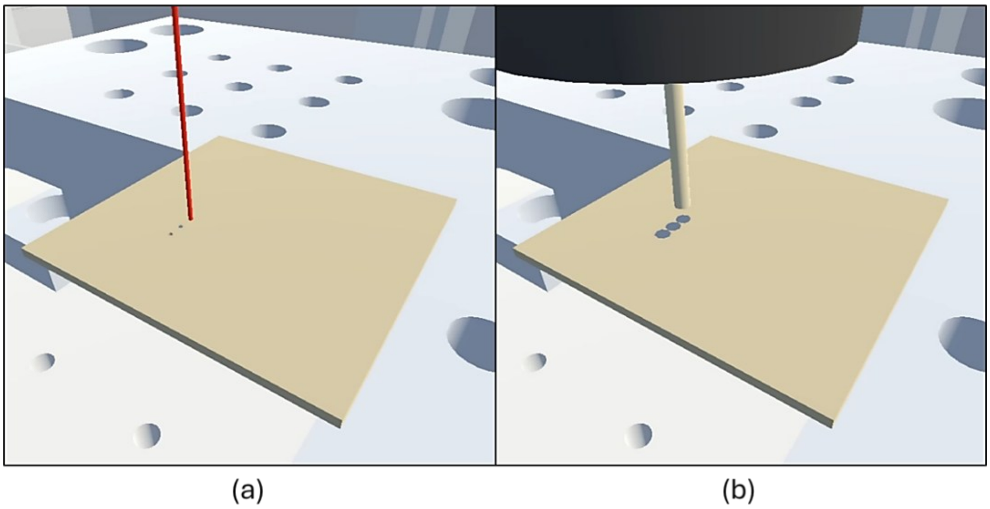

Figure 11. Visualization of sequential machining effects in the Digital Twin environment: (a) 300 μm diameter LBMM holes, (b) 500 μm diameter μEDM holes at the same locations.

4.2. Machining Time Estimation

The DT system can calculate machining times based on the G-code feed rate, as tool movement is governed by the feed rate specified in the G-code. However, calculating the machining time for the LBMM process is not feasible, as the actual processing time is recorded internally by the EZCAD software (closed system), which does not share data with the μEDM CNC controller software. Similarly, estimating machining time for the μEDM process is not possible using G-code feed rate alone, as μEDM machining time is stochastic and influenced by various factors such as material removal rate, discharge frequency, and spark stability. To address this, we include Z-displacement data from actual μEDM experiments to improve machining-time prediction.

Two sets of experiments were conducted to obtain the datasets: one for a 0.2 mm-thick and another for a 0.6 mm-thick stainless steel (SS304) workpiece, both machined at 90V and 10nF capacitance. These datasets enable the prediction of material removal for workpiece thicknesses between 0.2 and 0.6 mm. For this study, a thickness of 0.4 mm was selected for prediction, where a linear interpolation method was used to estimate its Z-depth profile and subsequently validate it against the corresponding 0.4 mm experimental data. Linear interpolation was used because the Z-depth data from the 0.2 mm and 0.6 mm workpieces show a similar and steady trend under the same machining conditions (90 V and 10 nF). Since no experimental data exist for intermediate thicknesses, interpolation provides a simple, practical way to estimate the Z-depth for the 0.4 mm workpiece. This allows a direct comparison with the actual experimental result for validation.

Figure 12 illustrates the comparison between the predicted and experimental Z-depth profiles for the 0.4 mm workpiece, with experimental Z-depth profiles in orange (0.2 mm), green (0.6 mm), and yellow (0.4 mm), and the predicted 0.4 mm profile shown in blue. It should be noted that, since the machining depth of the 0.2 mm workpiece is only 0.2 mm, the 0.2 mm data are linearly extrapolated to 0.04 mm prior to performing the 0.4 mm prediction. Then, the machining time was calculated by interpolating data from the 0.2 mm and 0.6 mm thickness profiles. To validate the prediction, an additional experiment was conducted using a 0.4 mm thick workpiece.

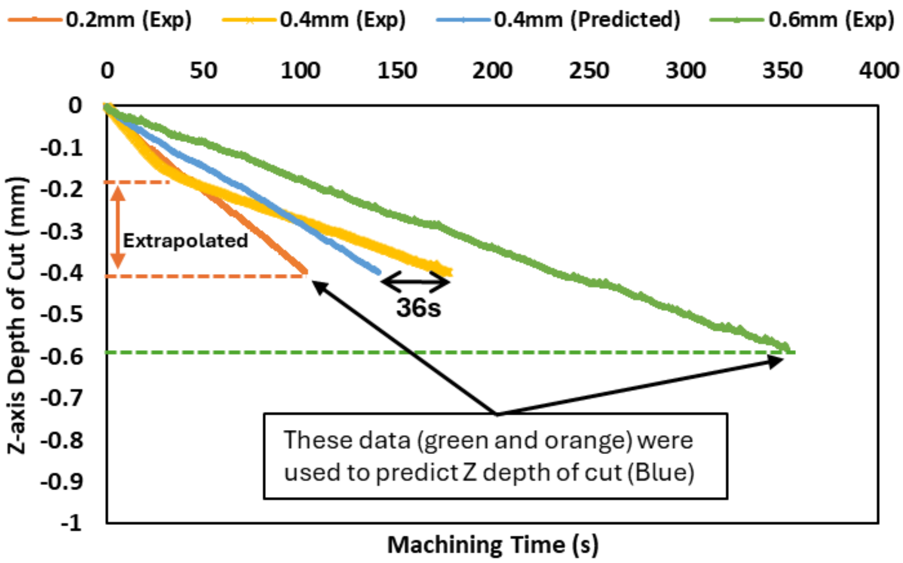

Figure 12. Comparison of predicted and actual Z-depth profiles for 0.4 mm workpiece thickness, predicted based on interpolation from 0.2 mm and 0.6 mm real machining data.

The results show a close agreement between the predicted and experimental machining times, with a difference of approximately 36 s, corresponding to a 20.2% error and an overall prediction accuracy of 79.8%. Although the percentage error appears relatively high, µEDM is inherently a nonlinear and stochastic process. Unlike conventional machining processes, material removal in µEDM is governed by a sequence of discrete electrical discharges, each exhibiting random variations in discharge energy, plasma channel formation, ignition delay, and crater size. Consequently, the material removal rate (MRR) fluctuates continuously throughout machining and does not scale linearly with workpiece thickness or machining depth.

As machining progresses, several depth-dependent phenomena further contribute to the stochastic behavior. Electrode wear gradually tapers the tool, altering the effective tool geometry and spark gap. At greater depths, debris evacuation becomes increasingly difficult due to restricted flushing conditions, leading to unstable discharge conditions, secondary discharges, arcing, and occasional short circuits. These phenomena reduce machining efficiency and introduce additional variability in the instantaneous MRR. Furthermore, the servo control system continuously adjusts the tool position to maintain a stable discharge gap, resulting in variable feed rates and intermittent machining pauses that are difficult to predict using deterministic models.

Given these characteristics, achieving 79.8% prediction accuracy with an interpolation-based approach shows that the proposed method captures the overall machining trend despite the process's randomness. The predicted Z-depth profile closely follows the experimental profile, indicating that interpolation provides a practical and computationally efficient way to estimate machining time. Nevertheless, further improvements may be achieved by incorporating nonlinear depth-dependent correction factors, adaptive electrode wear compensation, or data-driven approaches such as artificial intelligence and machine learning models capable of learning the complex stochastic relationships between machining parameters, electrode wear, flushing conditions, and material removal behavior. Such enhancements could further reduce prediction error and improve the robustness of machining time estimation for μEDM applications.

5. CONCLUSION

In conclusion, a comprehensive Digital Twin (DT) framework for the sequential Laser Beam Micromachining (LBMM) and micro-EDM (μEDM) process is proposed to address critical challenges in collision detection and process coordination. Integrating Internet of Things (IoT) technology with a Unity3D-based virtual environment enables real-time monitoring and interactive visualization of the machining system. Through IoT connectivity established via Firebase, the system achieves a low average latency of 16 ms, supporting responsive collision detection.

Unlike conventional point-based or bounding-box proximity checks, this method uses well-positioned 3D box colliders that reflect the actual tool and machine geometry, enhancing the realism and accuracy of collision detection. In addition to real-time monitoring, the DT framework supports offline process coordination through virtual simulation. Users can preview and validate the whole sequence of machining operations using G-code and M-code commands, visually assess tool-path execution, and estimate machining time. The results show a close match, with only a slight difference in overall machining time of approximately 36 seconds, corresponding to a 79.8% prediction accuracy. Mitigation: Simulated cutting effects, such as through-holes corresponding to LBMM and μEDM operations, enhance process interpretability. By incorporating real experimental Z-displacement data, the DT also demonstrates predictive capability for machining outcomes, illustrating its potential for future integration with AI-driven models. The DT eliminates the need for live camera feeds by enabling flexible, low-bandwidth, multi-angle visualization without added hardware costs.

The main limitation of this study for real-time collision detection is its reliance on geometry-based box colliders, which may not fully capture complex dynamic effects such as vibration, tool deflection, or rapid transient movements during high-speed machining. For machining time prediction, a key limitation is the use of a simplified interpolation-based approach, which does not fully account for the nonlinear and stochastic nature of μEDM material removal, reducing accuracy under varying machining conditions. For future improvements, more advanced physics-based collision models or sensor-assisted detection can be introduced to improve realism and accuracy, while data-driven or machine learning models can be developed to better capture nonlinear machining behavior and enhance the prediction of machining time under different process conditions.

The findings support the main objective by demonstrating that the developed Digital Twin framework successfully enables real-time analysis and decision-making for sequential machining. The low communication latency (16 ms) confirms its capability for real-time data exchange, while the synchronized 3D simulation and collision detection validate improved process coordination and safety. In addition, the online virtual environment and 79.8% machining time prediction accuracy show that the framework can perform effective virtual validation of LBMM–μEDM operations, fulfilling the intended objectives of monitoring, coordination, and predictive assessment.

ACKNOWLEDGMENT

This research is also funded under the grant PRGS/1/2022/TK03/UIAM/02/1 provided by the Ministry of Higher Education, Malaysia. Wan Ahmad Bin Wan Azhar is supported by the

KOE IIUM Engineering Merit Scholarship (KOEiems 2023). The data that support the findings of this study are available from the corresponding author upon request.

REFERENCES

[1] Li ZY, Wei XT, Guo YB, Sealy MP. (2015) State-of-art, challenges, and outlook on manufacturing of cooling holes for turbine blades. Mach. Sci. Technol., 19(3):361-399. https://doi.org/10.1080/10910344.2015.1051543

[2] Shang J, et al. (2023) Micro-hole array sprayer combined with an organic membrane to assist LIBS (MASOM-LIBS): A novel highly sensitive detection method for dissolved trace heavy metals in water. Talanta, 264:124780. https://doi.org/10.1016/j.talanta.2023.124780

[3] Wang C, Lu Z, Zhang K. (2018) Fabrication of micro-parts with high-aspect ratio micro-hole array by micro-powder injection molding. Materials, 11(10):1864. https://doi.org/10.3390/ma11101864

[4] Xu Z, Wang Y. (2021) Electrochemical machining of complex components of aero-engines: Developments, trends, and technological advances. Chinese J. Aeronaut., 34(2):28-53. https://doi.org/10.1016/j.cja.2019.09.016

[5] Davim JP. (2013) Nontraditional Machining Processes, 1st Ed. Springer London. https://doi.org/10.1007/978-1-4471-5179-1

[6] Zhang N, Wang M, Ban M, Guo L, Liu W. (2024) Femtosecond laser drilling 100 μm diameter micro holes with aspect ratios in a Nickel based superalloy. J. Mater. Res. Technol., 28:1415-1422. https://doi.org/10.1016/j.jmrt.2023.12.049

[7] Yung-Chou H. (2024) Applying punching without die to micro-hole array processing. J. Manuf. Process., 116:284-292. https://doi.org/10.1016/j.jmapro.2024.02.064

[8] Chavoshi SZ, Luo X. (2015) Hybrid micro-machining processes: A review. Precis. Eng., 41:1-23. https://doi.org/10.1016/j.precisioneng.2015.03.001

[9] Li L, Diver C, Atkinson J, Giedl-Wagner R, Helml HJ. (2006) Sequential laser and EDM micro-drilling for next generation fuel injection nozzle manufacture. CIRP Ann., 55(1):179-182. https://doi.org/10.1016/S0007-8506(07)60393-X

[10] Kim S, Kim BH, Chung DK, Shin HS, Chu CN. (2010) Hybrid micromachining using a nanosecond pulsed laser and micro EDM. J. Micromechanics Microengineering, 20(1):015037. https://doi.org/10.1088/0960-1317/20/1/015037

[11] Racz SG, Breaz RE, Cioca LI. (2020) Hazards that can affect CNC machine tools during operation—An AHP approach. Safety, 6(1):10. https://doi.org/10.3390/safety6010010

[12] Chen L, Xu K, Tang K. (2018) Optimized sequence planning for multi-axis hybrid machining of complex geometries. Comput. Graph., 70:176-187. https://doi.org/10.1016/j.cag.2017.07.018

[13] Basinger K, Webster C, Keough C, Wysk R, Harrysson O. (2020) Advanced manufacturing using linked processes: Hybrid manufacturing. In: Mass Production Processes, IntechOpen. https://doi.org/10.5772/intechopen.88560

[14] Cortina M, Arrizubieta JI, Ruiz JE, Ukar E, Lamikiz A. (2018) Latest developments in industrial hybrid machine tools that combine additive and subtractive operations. Materials, 11(12):2583. https://doi.org/10.3390/ma11122583

[15] Christiand, Kiswanto G. (2020) Digital twin approach for tool wear monitoring of micro-milling. Procedia CIRP, 93:1532-1537. https://doi.org/10.1016/j.procir.2020.03.140

[16] He Y, Guo J, Zheng X. (2018) From surveillance to digital twin: Challenges and recent advances of signal processing for industrial Internet of Things. IEEE Signal Process. Mag., 35(5):120-129. https://doi.org/10.1109/MSP.2018.2842228

[17] Wright L, Davidson S. (2020) How to tell the difference between a model and a digital twin. Adv. Model. Simul. Eng. Sci., 7(1):13. https://doi.org/10.1186/s40323-020-00147-4

[18] Semeraro C, Lezoche M, Panetto H, Dassisti M. (2021) Digital twin paradigm: A systematic literature review. Comput. Ind., 130:103469. https://doi.org/10.1016/j.compind.2021.103469

[19] Liu M, Fang S, Dong H, Xu C. (2021) Review of digital twin about concepts, technologies, and industrial applications. J. Manuf. Syst., 58:346-361. https://doi.org/10.1016/j.jmsy.2020.06.017

[20] Liu K, Song L, Han W, Cui Y, Wang Y. (2022) Time-varying error prediction and compensation for movement axis of CNC machine tool based on digital twin. IEEE Trans. Ind. Informatics, 18(1):109-118. https://doi.org/10.1109/TII.2021.3073649

[21] Almeida S, Mo JPT, Bil C, Ding S, Cheng CT. (2023) A novel robotic EDM digital twin for offline cutting-path programming. https://doi.org/10.3233/ATDE230624

[22] Wan Azhar WAB, Saleh T. (2025) An integrated setup for sequential hybrid laser beam micromachining (LBMM) and micro-EDM for machining micro-hole arrays with automated tool localization. Int. J. Precis. Eng. Manuf., 26(8):1889-1906. https://doi.org/10.1007/s12541-025-01251-4

[23] Wan Azhar WAB, Saleh T. (2025) Radial tool wear analysis and compensation strategy for microhole arrays in sequential hybrid laser beam micromachining (LBMM) and micro-EDM. Int. J. Adv. Manuf. Technol., 141(5-6):3411-3430. https://doi.org/10.1007/s00170-025-16717-y